Front. Med. 2025, 19(6): 1131−1143
https://doi.org/10.1007/s11684-025-1187-6

RESEARCH ARTICLE

Prognostic utility of baseline ASCL1/INSM1 expression and neutrophil-lymphocyte ratio in unresectable SCLC treated with first-line chemoimmunotherapy with or without radiotherapy

Yanli Zhu[1,*], Sheng Li[2,*], Hanxiao Chen[2,*], Guangqian Ji[3,*], Haiyue Wang[1], Xinting Diao[1], Xiuli Ma[1], Minglei Zhuo (✉)[2], Dongmei Lin (✉)[1]

[1]Key laboratory of Carcinogenesis and Translational Research (Ministry of Education), Department of Pathology, Peking University Cancer Hospital & Institute, Beijing 100142, China; [2]Key laboratory of Carcinogenesis and Translational Research (Ministry of Education), Department I of Thoracic Oncology, Peking University Cancer Hospital & Institute, Beijing 100142, China; [3]Department of Radiation Oncology, National Cancer Center/National Clinical Research Center for Cancer/Cancer Hospital, Chinese Academy of Medical Sciences and Peking Union Medical College, Beijing 100021, China

Abstract **While immune checkpoint inhibitors have revolutionized small cell lung carcinoma (SCLC) management, clinical benefits remain restricted to a subset of patients. This study investigates baseline biomarkers for predicting outcomes in unresectable SCLC patients receiving first-line chemoimmunotherapy with or without radiotherapy. We retrospectively analyzed treatment-naïve, unresectable SCLC patients undergoing first-line chemoimmunotherapy at Peking University Cancer Hospital (between June 2020 and November 2022). Clinicopathological parameters, pretreatment hematologic indices, and immunohistochemical profiles (ASCL1, NEUROD1, POU2F3, YAP1, PD-L1, CD8, MHC-I, and Rb) were correlated with survival outcomes using Cox proportional hazards models. Composite biomarker strategies were evaluated for therapeutic stratification. A total of 143 SCLC patients were included (LS=41, ES=102). The SCLC-A subtype demonstrated optimal median overall survival (OS) than other subtypes (18 months vs. 11 months, $P = 0.02$), and SCLC-P patients exhibited poorer prognosis than NE phenotypes (SCLC-A, SCLC-N, SCLC-AN). Multivariate analysis identified VALSG stage ($P = 0.02$) and bone metastases ($P = 0.045$) as independent OS predictors in the entire cohort. Patients stratified by ASCL1/INSM1 positivity and NLR thresholds showed markedly divergent outcomes, with $ASCL1^{+}/NLR^{low}$ group and or $INSM1^{+}/NLR^{low}$ group achieving superior OS in the overall cohort, LS-SCLC, and ES-SCLC. The ASCL1/INSM1-NLR composite biomarker stratifies survival outcomes for unresectable SCLC patients treated with first-line chemoimmunotherapy with or without radiotherapy. Prospective multicenter validation is required.**

Keywords small cell lung carcinoma; SCLC; molecular subtype; neutrophil-to-lymphocyte ratio; NLR; chemoimmunotherapy; prognosis

Introduction

Small cell lung carcinoma (SCLC), a high-grade neuroendocrine malignancy, accounts for 13%–15% of newly diagnosed pulmonary malignancies [1]. The advent of immune checkpoint inhibitors (ICIs), particularly anti-programmed death-1/programmed death-ligand 1 (PD-1/PD-L1) therapy, has engendered a paradigm-shifting advancement in the therapeutic algorithm for extensive-stage SCLC (ES-SCLC) [2–4]. Notably, the US Food and Drug Administration (FDA) approval has been granted for durvalumab consolidation therapy in limited-stage SCLC (LS-SCLC) patients achieving disease control after platinum-based concurrent chemoradiotherapy. Nevertheless, a substantial proportion of patients exhibit primary resistance to immunotherapy [2,3]. This clinical conundrum underscores the imperative to identify predictive biomarkers with both prognostic validity and therapeutic

Received June 11, 2025; accepted September 19, 2025
Correspondence: Dongmei Lin, lindm3@bjmu.edu.cn;
Minglei Zhuo, minglei1978@163.com

*Yanli Zhu, Sheng Li, Hanxiao Chen, and Guangqian Ji contributed equally to this work.

implications, which may catalyze the implementation of precision oncology strategies in SCLC management.

Emerging research into SCLC biology has established molecular subtypes (achaete-scute family BHLH transcription factor 1 (ASCL1), neuronal differentiation factor 1 (NEUROD1), POU class 2 homeobox 3 (POU2F3), Yes-associated protein 1 (YAP1)), driving exploration of subtype-specific therapeutic targets and predictive biomarkers, with potential implications for ICIs efficacy [5–8]. Transcriptional regulators *ASCL1*, *POU2F3*, and *YAP1* were among the genes identified to predict chemo-immunotherapy efficacy in ES-SCLC [9]. However, clinical validation of the predictive utility of these subtypes for immunotherapy remains inconclusive [7,10–15], underscoring their insufficiency as singular biomarkers. Additionally, molecular profiling faces technical hurdles due to frequent specimen limitations (e.g., scant biopsies with necrosis), necessitating development of practical biomarkers for real-world clinical application.

Recent evidence implicates the tumor immune microenvironment (TIME) as a predictive biomarker for immunotherapy response [16,17]. In SCLC, tumor-infiltrating lymphocyte (TIL) density and antigen-presenting machinery efficacy have emerged as prognostic indicators across therapeutic modalities [10,18–20]. Notably, systemic immune parameters (e.g., lactate dehydrogenase (LDH), neutrophil-to-lymphocyte ratio (NLR), platelet-to-lymphocyte ratio (PLR), lung immune prognostic index (LIPI)) modulate local tumor immunity and correlate with adverse survival in ES-SCLC [21–25]. However, scant data exist regarding the utility of hematologic inflammatory markers for immunotherapy selection in LS-SCLC [26], and their specific prognostic utility in SCLC necessitates prospective validation. Integration of local and systemic immune profiling may enable comprehensive immune-monitoring to optimize therapeutic strategies.

In this study, we investigated non-surgical LS/ES-SCLC patients receiving first-line chemoimmunotherapy with or without radiotherapy to correlate baseline clinicopathological variables with survival outcomes. We further sought to identify readily deployable predictive biomarkers for treatment response in this non-operable population.

Materials and methods

Patient selection and data collection

This retrospective analysis evaluated consecutively enrolled SCLC biopsy specimens (June 2020–November 2022; n = 143) from Peking University Cancer Hospital. Inclusion criteria: (I) pathologically confirmed pure SCLC; (II) tumor-node-metastasis (TNM) stage IIb–IVb disease, with patients receiving ⩾ 2 cycles of first-line PD-(L)1 inhibitor-based immuno-chemotherapy; (III) viable tumor content (⩾ 100 neoplastic cells); (IV) with clear prognostic information, including progression-free survival (PFS) and overall survival (OS) data, which were either retrieved from electronic medical records or obtained via telephone interviews. Exclusion criteria: surgical intervention, combined SCLC, concurrent malignancies, or life-threatening comorbidities. Conducted per Declaration of Helsinki (2013 revision) with institutional review board approval (2023KT23). Individual consent for this retrospective analysis was waived.

Clinicopathological variables were retrospectively collected, including demographics (age/sex), smoking history, Eastern Cooperative Oncology Group (ECOG) performance status (PS), metastatic patterns (brain, liver, bone, or other), Veterans Administration Lung Cancer Study Group (VALSG) stage, TNM stage, systemic treatment regimens, and radiotherapy history. Baseline serum biomarkers included neutrophil, lymphocyte, platelet counts, and LDH. Inflammatory indices were calculated as: NLR = neutrophil count/lymphocyte count; PLR = platelet count/lymphocyte count [27,28].

The final follow-up occurred on April 12, 2025. OS was calculated from the date of therapy to the date of death, and PFS was calculated from the date of therapy to the date of the last clinical evidence of recurrence, progression, or death. PFS1/PFS2 represented duration from front-line or ⩾ second-line therapy initiation to progression/death within respective treatment epochs.

All cases underwent blinded re-evaluation by two senior pathologists (Y.Z., H.W.) using standardized immunohistochemical panels for differential diagnosis, including CK, CD56, chromogranin A (CgA), synaptophysin (Syn), LCA, TTF-1, Napsin A, P40, CK5/6, NUT, INI-1, and SMARCA4 (also known as BRG1). Diagnostic discordances were resolved through multi-observer microscopy conference.

Immunohistochemistry staining and digital image analysis

Formalin-fixed, paraffin-embedded specimens were sectioned at 4 μm for immunohistochemistry (IHC) profiling. Molecular subtyping markers (ASCL1, NEUROD1, POU2F3, YAP1), immune markers (PD-L1, CD8, MHC I), and Rb protein were stained per established protocols (detailed in Table S1) [29,30]. Dual independent blinded evaluation was performed by experienced pathologists (Y.Z., H.W.).

The quantitative histoscore (H-score, 0–300 scale) was applied to subtyping markers and MHC I, calculated as: (staining intensity (1–3)) × (percentage of positive tumor cells) [31]. As previously reported, an H-score ⩽ 10 was

considered negative, while an H-score > 10 was considered positive [32]. Rb status was categorized as positive/wild-type (heterogeneous nuclear expression) or negative/mutant-type (complete nuclear loss).

PD-L1 expression was assessed in both neoplastic and stromal compartments. Positivity threshold: ⩾ 1% membranous staining in tumor cells or immune cells [33]. Tumor Proportion Score (TPS) quantified viable tumor cells with partial or complete membrane staining (⩾ 100 cells assessed). Combined Positive Score (CPS) calculated as (PD-L1$^+$ (cells tumor, lymphocytes, macrophages)/total viable tumor cells) × 100 [34].

Digital quantification of CD8$^+$ TILs was performed using whole-slide imaging (Pannoramic 250 Flash III scanner (3DHISTECH, Budapest, Hungary)) with QuPath (version 0.5.1). 3,3'-diaminobenzidine (DAB)-positive cells within tumor nests were enumerated [35]. Whole-slide averages were computed for statistical analysis.

Statistical analysis

Statistical analyses employed SPSS version 26.0 and GraphPad Prism version 8.0. Receiver operating characteristic (ROC) curves were generated to determine the area under the curve (AUC) values of the hematologic and pathological parameters, as well as their sensitivity and specificity at the cutoff values, and the optimal cutoff value was determined by ROC curve analysis as the points at which the Youden index (sensitivity + specificity – 1) values were maximal, using OS as the endpoint. Bonferroni adjustment was applied in post hoc subgroup biomarker analyses where appropriate. Molecular subtyping was achieved through unsupervised hierarchical clustering (ComplexHeatmap R package version 3.6.3) of subtype-defining transcription factor H-scores (ASCL1, NEUROD1, POU2F3, YAP1). Categorical variables were expressed as frequencies (%); continuous variables as medians (ranges). Intervariable associations utilized Chi-square/Fisher's exact tests (categorical) or Mann–Whitney U/Kruskal–Wallis tests (non-parametric). Spearman's rho assessed monotonic associations. Cox proportional hazards models identified prognostic factors (reported as hazard ratios (HRs) with 95% CIs). To mitigate the risk of overfitting in multivariable Cox regression models, we adopted a two-step approach: first, candidate variables were screened via univariate analysis with a liberal threshold ($P < 0.1$); second, multicollinearity among covariates was assessed using the variance inflation factor (VIF), and redundant variables were excluded. We also ensured an adequate number of events per variable (EPV > 10) to support model stability. VALSG stage and radiotherapy use were included as design/confounding variables to reduce treatment-selection bias. Model stability and optimism were assessed via bootstrap resampling (1000 iterations) to obtain 95% CIs for HRs and optimism-corrected C-indices. While Bonferroni correction is not routinely applied in multivariable Cox models—since they estimate independent effects —we emphasize that only variables with clinical or statistical relevance were retained, and HRs were interpreted conservatively in light of the study's retrospective design. Kaplan–Meier estimates with Log-rank testing were used to compare intergroup survival. For Kaplan–Meier analyses involving more than two groups, we used an overall Log-rank test to assess survival differences across subgroups. Since no pairwise comparisons were performed, multiple testing correction (e.g., Bonferroni) was not applied to the survival curves. To control for type I error due to multiple comparisons, Bonferroni correction was applied where appropriate, particularly in Kaplan–Meier survival analyses and ROC curve-based subgroup evaluations involving multiple biomarker combinations (e.g., ASCL1/NLR, INSM1/NLR). The corrected significance threshold was calculated as α/n, where n is the number of comparisons. For exploratory univariate Cox proportional hazards analyses, unadjusted P-values were reported, and results were interpreted cautiously in the context of biological plausibility. All statistical tests were two-sided, with $P < 0.05$ (or Bonferroni-corrected threshold) considered statistically significant.

Results

Baseline clinicodemographic profile

This cohort comprised 143 non-operable SCLC patients (LS = 41; ES = 102) undergoing first-line chemoimmunotherapy with or without radiotherapy. As shown in Table S2, the median age was 62 years (range, 36–79 years). The patients included were mostly male individuals (81.1%), and current or former smokers (78.3%). The ECOG PS at the start of treatment was 0–1 in 94.4% (n = 135) and greater than or equal to 2 in 5.6% (n = 8) of the patients. The most common sites of metastatic disease at diagnosis were liver, brain, and bone, accounting for 28.7% (n = 41), 13.3% (n = 19), and 32.9% (n = 47), respectively. 78 patients (54.5%) were treated with combined radiation therapy. All received platinum-based chemoimmunotherapy with PD-(L)1 inhibitors (PD-L1 inhibitors 74.8% (107/143); PD-1 inhibitors 25.2% (36/143)), including 5.6% (8/143) receiving anti-T cell immunoglobulin and the immunoreceptor tyrosine-based inhibitory motif domain (TIGIT) add-on therapy. We obtained information on the ⩾ second-line treatment for 70 patients (49.0%, 70/143), and the data was unavailable in 73 cases (51.0%). Among the 70 patients, most patients received combined treatment including chemotherapy and anti-angiogenic targeted therapy in the ⩾ second-line treatment, about

half of the patients (33/70) received additional immunotherapy, and only one patient was conducted radiotherapy.

Prognostic correlates of hematologic/pathologic parameters

Spearman analysis revealed inverse correlations between baseline hematologic indices (LDH: rho = −0.286, P = 0.001; NLR: rho = −0.227, P = 0.007) and OS, along with POU2F3 H-score negativity (rho = −0.203, P = 0.02). Conversely, $CD8^+$ TIL density showed positive OS association (rho = 0.195, P = 0.02). No other parameters reached statistical significance (Fig. 1).

ROC analysis demonstrated hematologic indices' modest discriminatory capacity (AUC > 0.5), with NLR exhibiting optimal performance (AUC = 0.66; sensitivity 56.7%, specificity 76.7% at the cutoff value of 3.21). $CD8^+$ TIL density achieved marginal predictive value (AUC = 0.61), while other pathologic markers showed limited utility (AUC < 0.6) (Fig. 2A–2C). Youden index optimization established critical thresholds: LDH = 283 U/L, NLR = 3.21, PLR = 155.2, and $CD8^+$ TILs = 150 cells/mm^2.

Molecular subtyping and prognostic significance

Unsupervised hierarchical clustering of IHC expression levels for four molecular markers (ASCL1, NEUROD1, POU2F3, YAP1) identified five SCLC subtypes. In addition to the previously characterized subtypes — ASCL1-dominant (SCLC-A), NEUROD1-dominant (SCLC-N), POU2F3-dominant (SCLC-P), and quadruple-negative (SCLC-QN) —a rare SCLC-AN subtype (ASCL1/NEUROD1 co-dominant) was identified, with limited prior reports (Fig. 3A). Subtype distribution was: SCLC-A (76.2%, n = 109), SCLC-N (6.3%, n = 9), SCLC-P (7.7%, n = 11), SCLC-QN (1.4%, n = 2), and SCLC-AN (8.4%, n = 12). Representative histopathological features of each subtype are illustrated in Fig. 3B. Kaplan–Meier analysis revealed SCLC-A patients exhibited the most favorable OS than other subtypes (18 months vs. 11 months, P = 0.02) (Fig. 3C and 3D), and SCLC-P patients exhibited poorer prognosis than NE phenotypes (SCLC-A, SCLC-N, SCLC-AN) (Fig. 3C).

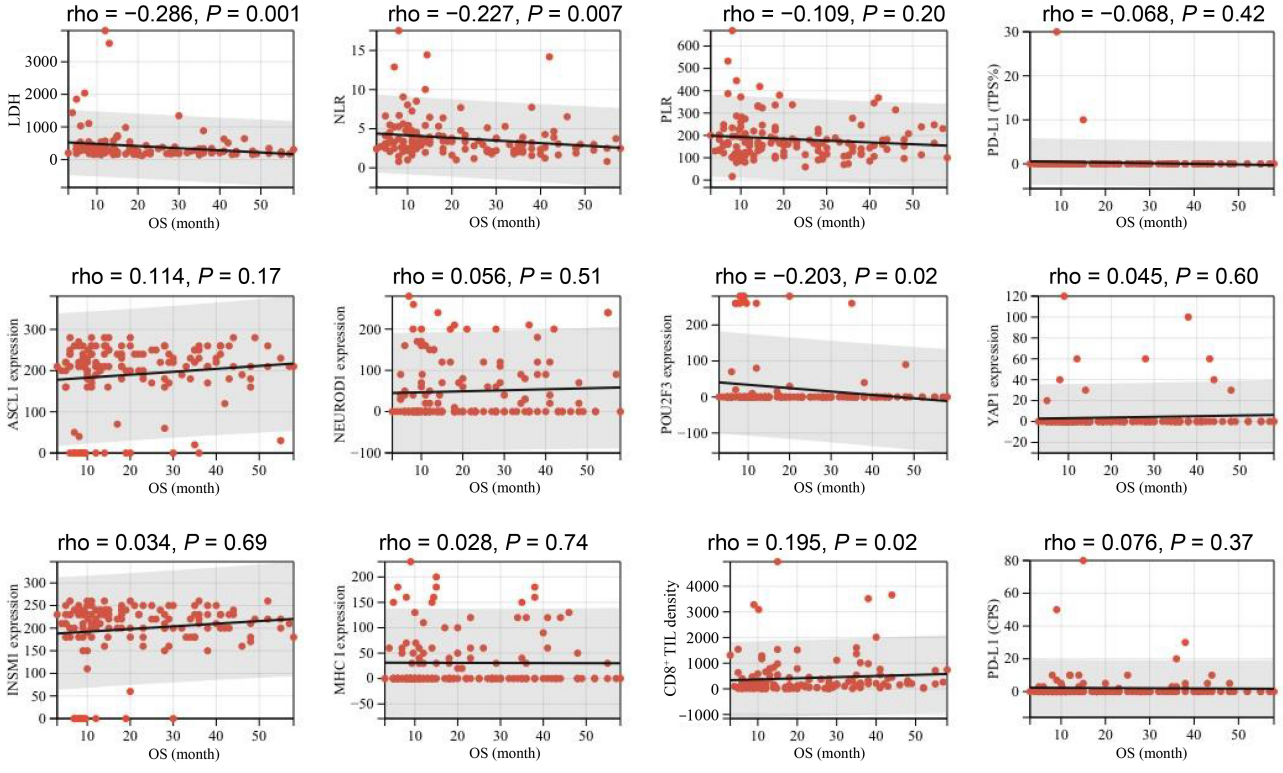

Fig. 1 Correlations of baseline hematologic indices/immunohistochemical profiles and OS time. Spearman analysis revealed inverse correlations between pretreatment hematologic indices (LDH: rho = −0.286, P = 0.001; NLR: rho = −0.227, P = 0.007) and OS, along with POU2F3 H-score negativity (rho = −0.203, P = 0.02). Conversely, $CD8^+$ TIL density showed positive OS association (rho = 0.195, P = 0.02). No other parameters reached statistical significance. OS, overall survival; LDH, lactate dehydrogenase; NLR, neutrophil-to-lymphocyte ratio; PLR, platelet-to-lymphocyte ratio; ASCL1, achaete-scute family BHLH transcription factor 1; NEUROD1, neuronal differentiation 1; POU2F3, POU class 2 homeobox 3; YAP1, Yes1-associated transcriptional regulator; H-score, histoscore; PD-L1, programmed death-ligand 1; TPS, Tumor Proportion Score; CPS, Combined Positive Score; MHC I, major histocompatibility complex class I; TIL, tumor-infiltrating lymphocyte.

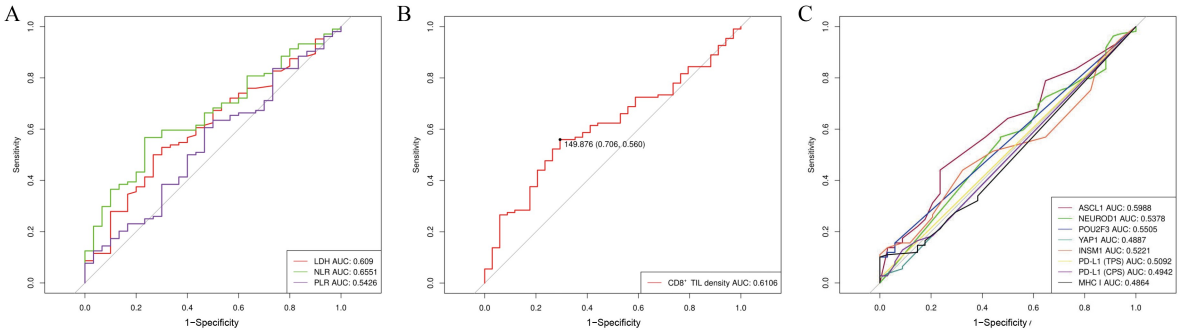

Fig. 2 ROC analysis of the hematologic and pathological parameters for predicting OS. (A) ROC analysis demonstrated hematologic indices' modest discriminatory capacity (AUC > 0.5), with NLR exhibiting the optimal performance (AUC = 0.66). (B) $CD8^+$ TIL density achieved marginal predictive value (AUC = 0.61; sensitivity 70.6%, specificity 56.0% at the cutoff value of 150). (C) Pathologic markers showed limited utility for predicting OS (AUC < 0.6). ROC, receiver operating characteristic; OS, overall survival; AUC, area under the curve; LDH, lactate dehydrogenase; NLR, neutrophil-to-lymphocyte ratio; PLR, platelet-to-lymphocyte ratio; TIL, tumor-infiltrating lymphocyte; ASCL1, achaete-scute family BHLH transcription factor 1; NEUROD1, neuronal differentiation 1; POU2F3, POU class 2 homeobox 3; YAP1, Yes1-associated transcriptional regulator; H-score, histoscore; PD-L1, programmed death-ligand 1; TPS, Tumor Proportion Score; CPS, Combined Positive Score; MHC I, major histocompatibility complex class I.

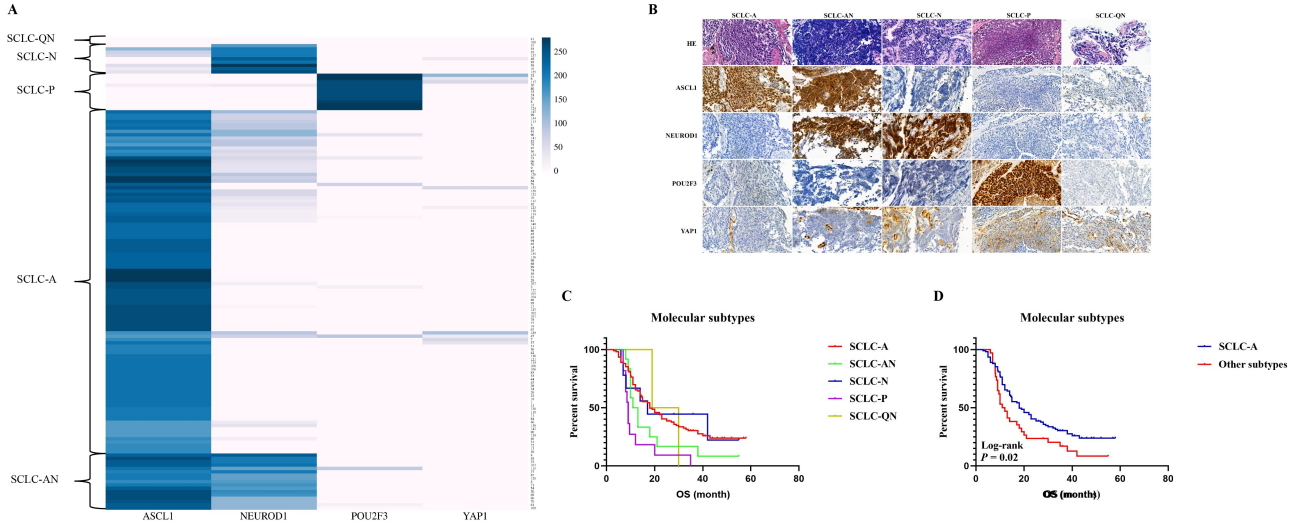

Fig. 3 Molecular subtyping and its prognostic significance. (A) Unsupervised hierarchical clustering of IHC expression levels for four molecular markers (ASCL1, NEUROD1, POU2F3, YAP1) identified five SCLC subtypes, including ASCL1-dominant (SCLC-A), NEUROD1-dominant (SCLC-N), POU2F3-dominant (SCLC-P), quadruple-negative (SCLC-QN), and ASCL1/NEUROD1 co-dominant (SCLC-AN). (B) Representative histopathological images of SCLC by molecular subtypes (×400). (C) Kaplan–Meier analysis revealed SCLC-A patients exhibited the most favorable OS, and SCLC-P patients exhibited poorer prognosis than those with NE phenotypes (SCLC-A, SCLC-N, SCLC-AN). (D) SCLC-A demonstrated optimal median overall survival (OS) than other subtypes (18 months vs. 11 months, $P = 0.02$). HE, hematoxylin and eosin; ASCL1, achaete-scute family BHLH transcription factor 1; NEUROD1, neuronal differentiation 1; POU2F3, POU class 2 homeobox 3; YAP1, Yes1-associated transcriptional regulator; OS, overall survival.

Survival analysis in relation to clinicopathological parameters in the entire cohort

All patients underwent routine follow-up until the data cutoff (April 12, 2025), with a median follow-up duration of 17 months (range: 3–58 months) for the entire cohort and 38 months (range: 26–58 months) for surviving patients. The median PFS1, PFS2, and OS were 7, 8, and 17 months, respectively. Disease progression occurred in 134 patients (93.7%), and 109 patients (76.2%) died during follow-up.

Univariable Cox regression analysis identified 12 clinicopathological parameters significantly associated with PFS1, PFS2, and OS ($P < 0.05$): VALSG stage, N stage, serum LDH, NLR, liver/bone metastases, radiotherapy, ASCL1/POU2F3 expression, NE differentiation, INSM1 expression, and $CD8^+$ TIL density (Table 1). Kaplan–Meier risk stratification across these

Table 1 Univariate analyses for prognostic significance of clinicopathologic parameters in the entire cohort

Clinicopathologic parameters	PFS1		PFS2		OS	
	P value	HR (95% CI)	*P* value	HR (95% CI)	*P* value	HR (95% CI)
Age, ⩽65 vs. > 65 years	0.29	0.819 (0.564–1.189)	0.41	0.861 (0.602–1.232)	0.20	0.773 (0.523–1.142)
Sex, male vs. female	0.87	1.039 (0.653–1.654)	0.20	1.341 (0.858–2.098)	0.44	1.217 (0.740–2.000)
Smoking story, no vs. yes	0.77	1.068 (0.686–1.664)	0.75	0.934 (0.616–1.416)	0.39	0.812 (0.507–1.301)
VALSG stage, LS vs.ES	**< 0.001**	0.418 (0.269–0.649)	**0.001**	0.504 (0.339–0.748)	**< 0.001**	0.282 (0.170–0.468)
T stage, 1–2 vs. 3–4	0.40	0.845 (0.572–1.248)	0.22	0.792 (0.546–1.149)	0.40	0.839 (0.558–1.264)
N stage, 0–2 vs. 3	0.053	0.692 (0.476–1.005)	**0.01**	0.642 (0.451–0.914)	**0.007**	0.577 (0.388–0.857)
ECOG PS, 0–1 vs. ⩾2	0.18	0.592 (0.275–1.278)	0.66	0.843 (0.393–1.807)	0.72	0.859 (0.377–1.957)
LDH, low vs. high	**0.01**	0.607 (0.416–0.886)	**0.002**	0.568 (0.396–0.817)	**0.002**	0.539 (0.366–0.794)
NLR, low vs. high	**< 0.001**	0.489 (0.336–0.712)	**< 0.001**	0.496 (0.348–0.707)	**0.001**	0.504 (0.342–0.745)
PLR, low vs. high	0.06	0.703 (0.485–1.019)	0.08	0.733 (0.516–1.041)	0.15	0.750 (0.508–1.107)
Liver metastases, no vs. yes	**0.001**	0.521 (0.350–0.776)	**0.001**	0.504 (0.342–0.742)	**< 0.001**	0.465 (0.309–0.700)
Brain metastases, no vs. yes	0.59	1.159 (0.684–1.964)	0.33	1.286 (0.772–2.143)	0.73	1.105 (0.630–1.940)
Bone metastases, no vs. yes	**0.001**	0.510 (0.348–0.746)	**0.001**	0.548 (0.379–0.794)	**< 0.001**	0.376 (0.251–0.564)
Radiotherapy, no vs. yes	**< 0.001**	2.174 (1.508–3.132)	**< 0.001**	2.131 (1.506–3.016)	**< 0.001**	2.051 (1.402–2.999)
Anti-TIGIT antibody, no vs. yes	0.90	1.051 (0.490–2.258)	0.90	0.956 (0.467–1.957)	0.72	1.149 (0.533–2.475)
ICIs inhibitors, PD-L1 inhibitors vs. PD-1 inhibitors	0.12	1.410 (0.912–2.181)	0.11	1.392 (0.928–2.087)	0.054	1.586 (0.992–2.533)
⩾second-line immunotherapy, no vs. yes	0.19	1.393 (0.845–2.295)	0.14	1.444 (0.886–2.355)	0.37	1.261 (0.757–2.101)
ASCL1 expression, Neg vs. Pos	0.07	1.671 (0.951–2.936)	0.050	1.753 (0.999–3.076)	**0.005**	2.253 (1.276–3.977)
NEUROD1 expression, Neg vs. Pos	0.27	1.228 (0.852–1.769)	0.26	1.219 (0.864–1.720)	0.41	1.171 (0.801–1.712)
POU2F3 expression, Neg vs. Pos	0.36	0.788 (0.470–1.319)	0.18	0.710 (0.430–1.173)	**0.03**	0.544 (0.319–0.927)
YAP1 expression, Neg vs. Pos	0.33	1.428 (0.696–2.929)	0.57	1.205 (0.632–2.298)	0.54	1.268 (0.588–2.736)
NE differentiation, NE phenotype vs. non-NE phenotype	**0.02**	0.496 (0.276–0.892)	**0.005**	0.432 (0.239–0.781)	**0.005**	0.433 (0.241–0.778)
INSM1 expression, Neg vs. Pos	**0.008**	2.455 (1.270–4.748)	**0.002**	2.804 (1.445–5.443)	**0.002**	2.918 (1.505–5.658)
Rb expression, Neg vs. Pos	0.72	1.095 (0.670–1.788)	0.91	0.974 (0.620–1.530)	0.85	0.954 (0.575–1.582)
Tumor PD-L1 expression, Neg vs. Pos	0.94	0.947 (0.233–3.849)	0.80	0.832 (0.204–3.384)	0.26	0.444 (0.109–1.814)
Stromal PD-L1 expression, Neg vs. Pos	0.78	0.936 (0.589–1.487)	0.90	1.030 (0.666–1.593)	0.48	1.193 (0.734–1.939)
MHC Ⅰ expression, Neg vs. Pos	0.85	1.037 (0.712–1.511)	0.46	1.143 (0.799–1.636)	0.68	1.088 (0.732–1.618)
$CD8^+$ TIL density, low vs. high	0.08	1.376 (0.958–1.977)	**0.03**	1.458 (1.033–2.059)	**0.002**	1.820 (1.239–2.672)

SCLC, small cell lung carcinoma; PFS, progression-free survival; OS, overall survival; HR, hazard ratio; Pos, positive; Neg, negative; VALSG, Veterans Administration Lung Cancer Study Group; ECOG, Eastern Cooperative Oncology Group; LDH, lactate dehydrogenase; NLR, neutrophil-to-lymphocyte ratio; PLR, platelet-to-lymphocyte ratio; TIGIT, T cell immunoglobulin and the immunoreceptor tyrosine-based inhibitory motif domain; ICIs, immune checkpoint inhibitors; ASCL1, achaete-scute family BHLH transcription factor 1; NEUROD1, neuronal differentiation 1; POU2F3, POU class 2 homeobox 3; YAP1, Yes1-associated transcriptional regulator; NE, neuroendocrine; PD-L1, programmed death-ligand 1; MHC I, major histocompatibility complex class I; TIL, tumor-infiltrating lymphocyte.
Significant *P* values are highlighted in bold.

parameters demonstrated significant associations with OS (Fig. 4B).

Multivariable Cox regression analysis incorporating all 12 parameters confirmed the independent prognostic significance of VALSG stage (HR 0.502, 95% CI 0.276–0.913; $P = 0.02$) and bone metastases (HR 0.636, 95% CI 0.408–0.990; $P = 0.045$) for OS (Fig. 4A). Elevated NLR and radiotherapy administration independently predicted PFS1 and PFS2 outcomes (Fig. S1).

Survival analysis stratified by disease stage in LS- and ES-SCLC

Comparative analysis of clinicopathological parameters revealed elevated serum LDH ($P < 0.001$), NLR ($P = 0.001$), $CD8^+$ TIL density ($P = 0.02$), and radiotherapy frequency ($P < 0.001$) in ES-SCLC versus LS-SCLC patients, with no intergroup differences in other variables (Table S3). Next, univariate Cox regression analyses were performed in LS-SCLC (Table S4) and ES-SCLC patients

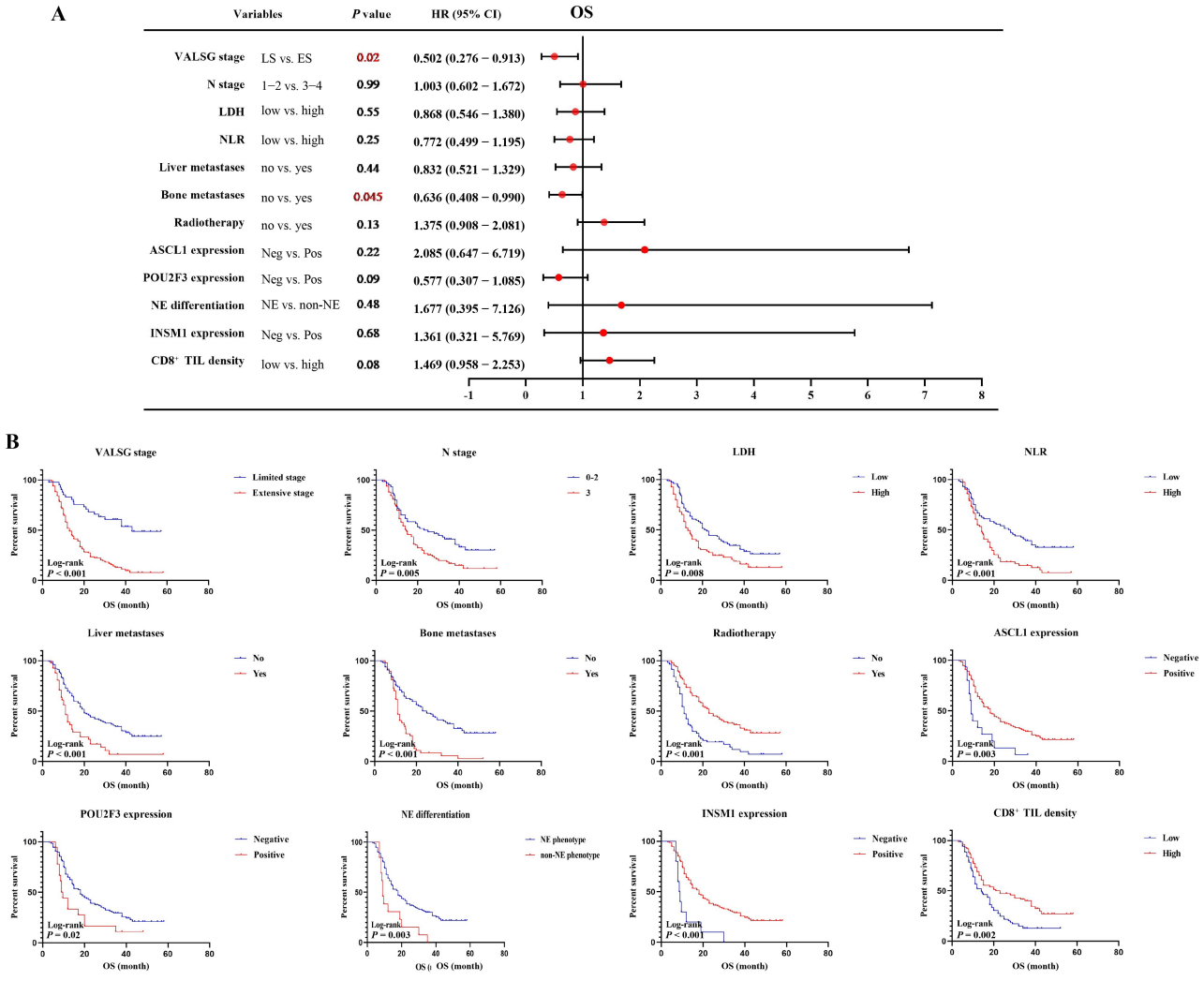

Fig. 4 Survival analysis in relation to clinicopathological parameters in the entire cohort. (A) The clinicopathologic parameters with statistically significant differences in univariate analyses were included in a multivariate Cox proportional hazards regression model, and the multivariable Cox analysis confirmed the independent prognostic significance of VALSG stage (HR 0.502, 95% CI 0.276–0.913; $P = 0.02$) and bone metastases (HR 0.636, 95% CI 0.408–0.990, $P = 0.045$) for OS. (B) Kaplan–Meier risk stratification demonstrated significant associations with OS across the parameters identified by univariate Cox analysis. VALSG, Veterans Administration Lung Cancer Study Group; LDH, lactate dehydrogenase; NLR, neutrophil-to-lymphocyte ratio; ASCL1, achaete-scute family BHLH transcription factor 1; POU2F3, POU class 2 homeobox 3; NE, neuroendocrine; TIL, tumor-infiltrating lymphocyte.

(Table S5), and clinicopathologic parameters with statistically significant differences in univariate analyses were included in a multivariate Cox proportional hazards regression model (Table S6). For the LS-SCLC patients, NE differentiation correlated with prolonged PFS1 (HR 0.246, 95% CI 0.071–0.848; $P = 0.03$), while non-receipt of radiotherapy independently predicted inferior survival (HR 3.960, 95% CI 1.373–11.419; $P = 0.01$). For the ES-SCLC patients, low NLR and radiotherapy administration were favorable predictors for PFS1/PFS2, and bone metastases conferred worse OS outcomes, which were consistent with cohort-wide trends.

Combined biomarkers predict outcomes in unresectable SCLC treated with first-line chemoimmunotherapy

Given the absence of standalone prognostic biomarkers across the entire cohort or within LS-/ES-SCLC subgroups, we evaluated combinatorial biomarkers integrating ASCL1 expression (negative/positive), INSM1 expression (negative/positive), NLR (low/high), and $CD8^+$ TIL density (low/high). Survival analysis stratified by these combinations revealed significant associations with OS (Figs. 5 and S2). Kaplan–Meier analysis showed significant differences in OS among the

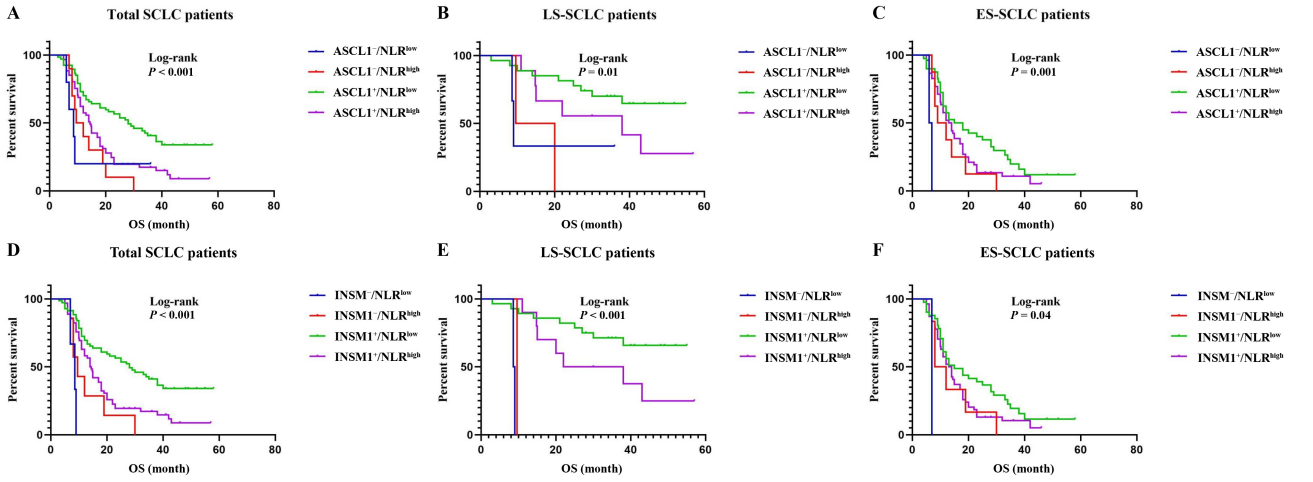

Fig. 5 Kaplan–Meier curves of OS according to four groups of the ASCL1/INSM1-NLR composite biomarker in the overall cohort, LS-SCLC, and ES-SCLC. (A–C) ASCL1/NLR stratification: ASCL1^{+}/NLR^{low} patients exhibited superior OS compared to other groups in the overall cohort ($P < 0.001$), LS-SCLC ($P = 0.01$), and ES-SCLC ($P = 0.001$). (D–F) INSM1/NLR stratification: INSM1^{+}/NLR^{low} patients demonstrated optimal survival outcomes across all subgroups in the overall cohort ($P < 0.001$), LS-SCLC ($P < 0.001$), and ES-SCLC ($P = 0.04$). SCLC, small cell lung carcinoma; ES-SCLC, extensive-stage SCLC; LS-SCLC, limited-stage SCLC; ASCL1, achaete-scute family BHLH transcription factor 1; NLR, neutrophil-to-lymphocyte ratio.

four ASCL1/NLR-defined subgroups in the overall cohort ($P < 0.001$), LS-SCLC ($P = 0.01$), and ES-SCLC ($P = 0.001$) (Fig. 5A–5C). Notably, patients with ASCL1^{+}/NLR^{low} profile appeared to have the most favorable survival curves. Similarly, OS significantly differed across the INSM1/NLR-defined subgroups in the overall cohort ($P < 0.001$), LS-SCLC ($P < 0.001$), and ES-SCLC ($P = 0.04$) (Fig. 5D–5F), with the INSM1^{+}/NLR^{low} group showing the most favorable survival curve. Key findings were as follows: (1) ASCL1/NLR stratification: ASCL1^{+}/NLR^{low} patients exhibited superior OS compared to other groups in the overall cohort ($P < 0.001$), LS-SCLC ($P = 0.01$), and ES-SCLC ($P = 0.001$) (Fig. 5A–5C); (2) INSM1/NLR stratification: INSM1^{+}/NLR^{low} patients demonstrated optimal survival outcomes across all subgroups in the overall cohort ($P < 0.001$), LS-SCLC ($P < 0.001$), and ES-SCLC ($P = 0.04$) (Fig. 5D–5F).

Discussion

First-line chemoimmunotherapy is now standard for ES-SCLC, and investigational efforts are now focused on integrating immunotherapy with concurrent chemoradiotherapy for LS-SCLC. However, given SCLC's marked molecular heterogeneity and the limited immunotherapy-responsive subpopulation, reliable predictive biomarkers remain an unmet clinical need. This retrospective cohort study evaluates the prognostic and predictive utility of clinicopathological parameters—including clinical profiles, hematologic indices, and immunohistochemical biomarkers —in unresectable SCLC patients receiving front-line chemoimmunotherapy.

In 2019, Rudin *et al*. established the molecular classification for SCLC, defining four subtypes—SCLC-A, SCLC-N, SCLC-P, and SCLC-Y —with distinct molecular profiles and therapeutic vulnerabilities, thereby advancing personalized treatment strategies [5]. Subsequently, Gay *et a*l. identified the SCLC-I subtype, marked by low ASCL1/NEUROD1/POU2F3 expression, enriched inflammatory gene signatures, and mesenchymal features, demonstrating enhanced responsiveness to ICIs [7]. Retrospective analysis of the IMpower-133 trial revealed a trend toward improved median OS in SCLC-I patients receiving atezolizumab versus chemotherapy (18.2 months vs. 10.4 months; HR 0.57, 95% CI 0.28–1.15), suggesting potential predictive utility of this subtype for ICI benefit [7]. These findings were corroborated by the CASPIAN trial, where SCLC-I tumors exhibited superior survival outcomes with immunotherapy [12]. In our cohort, no YAP1-driven (SCLC-Y) subtype was observed. Instead, we identified a quadruple-negative subtype (SCLC-QN, 1.4%, $n = 2$), potentially analogous to SCLC-I. However, unlike prior reports, SCLC-QN patients in our analysis showed no survival advantage over other subtypes (Fig. 3C), possibly due to the limited sample size ($n = 2$). Surprisingly, SCLC-A demonstrated optimal median OS than non-SCLC-A subtype (18 months vs. 11 months, $P = 0.02$).

We validated the existence of the SCLC-AN subtype (ASCL1/NEUROD1 co-dominant), corroborating prior reports [8,32,36–38]. Aligning with IMpower-133 trial retrospective analyses [7], SCLC-P patients exhibited

poorer prognosis than NE phenotypes (SCLC-A, SCLC-N, SCLC-AN) in our cohort. Paradoxically, emerging evidence highlights the SCLC-P subtype as the most immunogenically active [13,39]. Our previous whole-tissue spatial profiling of surgically resected SCLC tumors revealed enriched MHC I/II expression, elevated PD-L1 positivity, and inflamed tumor microenvironments ($CD8^+/CD3^+$ T cell infiltration) in SCLC-P compared to other subtypes [30]. Notably, Chen *et al*. further demonstrated that higher POU2F3 protein expression correlated with improved survival in immunotherapy or chemoimmunotherapy-treated patients [13]. These findings underscore an unresolved paradox: while SCLC-P tumors exhibit intrinsic immunogenic potential, their clinical outcomes remain suboptimal, suggesting a discordance between tumor immunogenicity and therapeutic efficacy.

Prior studies indicate that low NE SCLC exhibits enhanced immune cell infiltration, while high NE SCLC demonstrates immunosuppressive microenvironments with reduced infiltration, conferring differential immunotherapeutic susceptibility [5,7,40,41]. Emerging evidence reveals $ASCL1^+$ immunoreactive SCLC subsets display substantial NK/T cell infiltration in clinical specimens, confirming that immune-inflamed phenotypes may coexist across both NE and non-NE phenotypes [15]. The inflamed phenotype demonstrates variable prevalence across molecular subtypes [14]. Notably, recent clinical data identify a NE tumor subgroup with elevated T cell infiltration and diminished macrophage presence that shows a superior response to anti-PD-L1/chemotherapy combinations [15]. Collectively, these findings underscore tumor microenvironmental immune signatures as critical determinants of SCLC treatment outcomes and long-term survival [42].

Emerging evidence suggests $CD8^+$ TIL density correlates with survival outcomes in ES-SCLC patients receiving ICI monotherapy or chemoimmunotherapy combinations [10,43]. Immune classification systems incorporating $CD3^+/CD8^+$ lymphocyte spatial distribution patterns have shown predictive value for ICI responsiveness in relapsed disease [44]. Pasello *et al*. further established associations between spatially resolved immune cell architectures and first-line immunochemotherapy efficacy, emphasizing TIME dynamics and cellular crosstalk as determinants of therapeutic response and survival [45]. While our univariable Cox analysis identified $CD8^+$ TIL density as an independent prognostic factor for both PFS2 and OS (Table 1), multivariable adjustment attenuated these associations, showing no significant impact on PFS2 (Fig. S1) or OS (Fig. 4). Subgroup analyses across LS-SCLC and ES-SCLC cohorts confirmed limited prognostic utility of $CD8^+$ TIL density (Table S6, Fig. S2). Methodological variations likely explain these inconsistencies: (1) Heterogeneity in specimen types (biopsies *vs.* surgical resections; primary tumors vs. lymph node metastases), and biopsies and lymph node metastases potentially distorting immune cell distribution assessments; (2) Divergent analytical approaches, ranging from manual quantification to digital pathology platforms with inconsistent scoring thresholds. These findings challenge the translational potential of $CD8^+$ TIL density as a standalone predictive biomarker for SCLC treatment outcomes.

The immune microenvironment encompasses both TILs and systemic inflammatory components, demonstrating dynamic interplay through bidirectional cellular transformation [46]. Circulating immune cells serve as biomarkers of host immunological competence, capable of initiating and sustaining anti-tumor responses. Current evidence identifies LDH, NLR, PLR, and LIPI as established prognostic indicators for SCLC patients undergoing chemotherapy or immunotherapy [21–25]. Our univariate Cox regression analysis across the entire SCLC cohort demonstrated that baseline low-LDH ($\leqslant$ 283 U/L) and low NLR ($<$ 3.21) were significantly associated with prolonged PFS1 (HR 0.607, $P = 0.01$; HR 0.489, $P < 0.001$), PFS2 (HR 0.568, $P = 0.002$; HR 0.496, $P < 0.001$), and OS (HR 0.539, $P = 0.002$; HR 0.504, $P = 0.001$), whereas PLR showed no prognostic correlation (Table 1). VALSG stage-stratified analysis revealed low NLR as an independent predictor for favorable PFS outcomes in ES-SCLC (PFS1 HR 0.581, $P = 0.02$; PFS2 HR 0.515, $P = 0.005$; Table S6) and was associated with PFS1 in LS-SCLC (HR 0.409, $P = 0.03$; Table S4). While NLR emerged as the optimal hematological predictor for therapeutic response stratification, its lack of multivariate significance in the overall cohort suggests the necessity for composite biomarkers integrating NLR with complementary immunological indicators. Such combinatorial approaches may better characterize global immune status and optimize clinical decision-making in SCLC management.

A key finding of this study is the development and validation of composite prognostic biomarkers that holistically assess systemic immune status, potentially enhancing clinical decision-making for unresectable SCLC. Our analysis revealed that patients with either the $ASCL1^+/NLR^{low}$ or $INSM1^+/NLR^{low}$ profiles achieved superior survival outcomes when receiving first-line chemoimmunotherapy. The ASCL1/INSM1-NLR composite biomarker offers particular clinical value due to its cost-effectiveness, routine accessibility through standard IHC and complete blood counts, and potential utility in optimizing patient selection for immunotherapy regimens. While these findings require validation through prospective multicenter studies, they present a pragmatic approach to personalizing treatment strategies in unresectable SCLC management.

This study has several limitations. First, the retrospective single-center design inherently carries the risks of selection bias. Second, while we assembled a relatively large cohort of unresectable LS-SCLC patients receiving first-line chemoimmunotherapy, the modest cohort size may limit the statistical power for subgroup analyses. Third, the inclusion of clinically heterogeneous populations —including patients with ECOG PS 2, untreated brain metastases at diagnosis, and deviations from standard treatment protocols (e.g., abbreviated chemotherapy cycles or delayed radiotherapy) — introduces potential confounding variables, though this heterogeneity more accurately mirrors real-world clinical scenarios. Finally, the synergistic treatment design precludes definitive attribution of survival benefits to immunotherapy versus chemotherapy components. Despite these constraints, our findings provide clinically relevant insights into complex patient scenarios while generating testable hypotheses for prospective validation studies.

Conclusions

In summary, this study demonstrates the clinical validity of immunohistochemically defined SCLC molecular subtypes, with SCLC-A subtype exhibiting superior survival outcomes. Multivariate Cox regression confirmed VALSG staging and bone metastasis as independent prognostic factors for OS in chemoimmunotherapy-treated unresectable SCLC. Notably, we propose a composite predictive model that can be readily and universally obtained at a low cost in clinical practice, and either $ASCL1^{+}/NLR^{low}$ or $INSM1^{+}/NLR^{low}$ could be considered a stratifying criterion for first-line immuno-chemotherapy with or without radiotherapy of unresectable SCLC patients, including LS-SCLC and ES-SCLC patients. Further larger prospective studies are needed to validate the predictive value of the combined biomarker to establish its role in therapeutic decision-making frameworks.

Acknowledgements

This work was supported by the National Natural Science Foundation of China (82141117), Beijing Natural Science Foundation (L248048), Wu Jieping Medical Foundation (320.6750.2021-16-19), Clinical Research Fund for Distinguished Young Scholars of Beijing Cancer Hospital (QNJJ202212, QNJJ202403), Guangzhou Life Oasis Public Service Center Research and Exchange Program in the Field of Health (1-35), Beijing Xisike Clinical Oncology Research Foundation (Y-pierrefabre202101-0099), Beijing Vlove Charity Foundation (JYKY2024-0200426027), and the Science Foundation of Peking University Cancer Hospital (PY202303).

Compliance with ethics guidelines

Conflicts of interest Yanli Zhu, Sheng Li, Hanxiao Chen, Guangqian Ji, Haiyue Wang, Xinting Diao, Xiuli Ma, Minglei Zhuo, and Dongmei Lin declare no conflict of interest.

The study was approved by the Ethics Committee of Peking University Cancer Hospital and the local review board, and the study was performed in accordance with the ethical standards as laid down in the 1964 Declaration of Helsinki and its later amendments or comparable ethical standards. Informed consent was obtained from all patients for being included in the study.

Data availability and compliance statement

The authors declare that the acquisition and subsequent use of all data presented in this manuscript comply fully with all relevant local, national, and international laws, regulations, ethical guidelines (including the approval (No. 2023KT23) from the Ethics Committee of Peking University Cancer Hospital and the local review board), and the terms of use associated with the original data sources.

The authors bear full legal responsibility for ensuring the legality of data acquisition and all subsequent uses.

Electronic supplementary material Supplementary material is available in the online version of this article at https://doi.org/10.1007/s11684-025-1187-6 and is accessible for authorized users.

References

1. Siegel RL, Miller KD, Fuchs HE, Jemal A. Cancer statistics, 2022. CA Cancer J Clin 2022; 72(1): 7–33
2. Horn L, Mansfield AS, Szczęsna A, Havel L, Krzakowski M, Hochmair MJ, Huemer F, Losonczy G, Johnson ML, Nishio M, Reck M, Mok T, Lam S, Shames DS, Liu J, Ding B, Lopez-Chavez A, Kabbinavar F, Lin W, Sandler A, Liu SV. First-line atezolizumab plus chemotherapy in extensive-stage small-cell lung cancer. N Engl J Med 2018; 379(23): 2220–2229
3. Paz-Ares L, Dvorkin M, Chen Y, Reinmuth N, Hotta K, Trukhin D, Statsenko G, Hochmair MJ, Özgüroğlu M, Ji JH, Voitko O, Poltoratskiy A, Ponce S, Verderame F, Havel L, Bondarenko I, Kazarnowicz A, Losonczy G, Conev NV, Armstrong J, Byrne N, Shire N, Jiang H, Goldman JW; CASPIAN investigators. Durvalumab plus platinum-etoposide versus platinum-etoposide in first-line treatment of extensive-stage small-cell lung cancer (CASPIAN): a randomised, controlled, open-label, phase 3 trial. Lancet 2019; 394(10212): 1929–1939
4. Rudin CM, Awad MM, Navarro A, Gottfried M, Peters S, Csőszi T, Cheema PK, Rodriguez-Abreu D, Wollner M, Yang JC, Mazieres J, Orlandi FJ, Luft A, Gümüş M, Kato T, Kalemkerian GP, Luo Y, Ebiana V, Pietanza MC, Kim HR. Pembrolizumab or placebo plus etoposide and platinum as first-line therapy for extensive-stage small-cell lung Cancer: randomized, double-blind,

phase III KEYNOTE-604 study. J Clin Oncol 2020; 38(21): 2369–2379

5. Rudin CM, Poirier JT, Byers LA, Dive C, Dowlati A, George J, Heymach JV, Johnson JE, Lehman JM, MacPherson D, Massion PP, Minna JD, Oliver TG, Quaranta V, Sage J, Thomas RK, Vakoc CR, Gazdar AF. Molecular subtypes of small cell lung cancer: a synthesis of human and mouse model data. Nat Rev Cancer 2019; 19(5): 289–297
6. Owonikoko TK, Dwivedi B, Chen Z, Zhang C, Barwick B, Ernani V, Zhang G, Gilbert-Ross M, Carlisle J, Khuri FR, Curran WJ, Ivanov AA, Fu H, Lonial S, Ramalingam SS, Sun SY, Waller EK, Sica GL. YAP1 expression in SCLC defines a distinct subtype with T-cell-inflamed phenotype. J Thorac Oncol 2021; 16(3): 464–476
7. Gay CM, Stewart CA, Park EM, Diao L, Groves SM, Heeke S, Nabet BY, Fujimoto J, Solis LM, Lu W, Xi Y, Cardnell RJ, Wang Q, Fabbri G, Cargill KR, Vokes NI, Ramkumar K, Zhang B, Della CC, Robson P, Swisher SG, Roth JA, Glisson BS, Shames DS, Wistuba II, Wang J, Quaranta V, Minna J, Heymach JV, Byers LA. Patterns of transcription factor programs and immune pathway activation define four major subtypes of SCLC with distinct therapeutic vulnerabilities. Cancer Cell 2021; 39(3): 346–360.e7
8. Baine MK, Hsieh MS, Lai WV, Egger JV, Jungbluth AA, Daneshbod Y, Beras A, Spencer R, Lopardo J, Bodd F, Montecalvo J, Sauter JL, Chang JC, Buonocore DJ, Travis WD, Sen T, Poirier JT, Rudin CM, Rekhtman N. SCLC subtypes defined by ASCL1, NEUROD1, POU2F3, and YAP1: a comprehensive immunohistochemical and histopathologic characterization. J Thorac Oncol 2020; 15(12): 1823–1835
9. Fujimoto D, Shibaki R, Kimura K, Haratani K, Tamiya M, Kijima T, Sato Y, Hata A, Yokoyama T, Taniguchi Y, Uchida J, Tanaka H, Furuya N, Miura S, Onishi MI, Sakata S, Miyauchi E, Yamamoto N, Koh Y, Akamatsu H. Identification of key gene signatures for predicting chemo-immunotherapy efficacy in extensive-stage small-cell lung cancer using machine learning. Lung Cancer 2025; 199: 108079
10. Rudin CM, Balli D, Lai WV, Richards AL, Nguyen E, Egger JV, Choudhury NJ, Sen T, Chow A, Poirier JT, Geese WJ, Hellmann MD, Forslund A. Clinical benefit from immunotherapy in patients with SCLC is associated with tumor capacity for antigen presentation. J Thorac Oncol 2023; 18(9): 1222–1232
11. Schroeder BA, Thomas A. SCLC subtypes and biomarkers of the transformative immunotherapy responses. J Thorac Oncol 2023; 18(9): 1114–1117
12. Goldman JW, Dvorkin M, Chen Y, Reinmuth N, Hotta K, Trukhin D, Statsenko G, Hochmair MJ, Özgüroğlu M, Ji JH, Garassino MC, Voitko O, Poltoratskiy A, Ponce S, Verderame F, Havel L, Bondarenko I, Każarnowicz A, Losonczy G, Conev NV, Armstrong J, Byrne N, Thiyagarajah P, Jiang H, Paz-Ares L; CASPIAN investigators. Durvalumab, with or without tremelimumab, plus platinum-etoposide versus platinum-etoposide alone in first-line treatment of extensive-stage small-cell lung cancer (CASPIAN): updated results from a randomised, controlled, open-label, phase 3 trial. Lancet Oncol 2021; 22(1): 51–65
13. Chen Y, Fang Z, Tang Y, Jin Y, Guo C, Hu L, Xu Y, Ma X, Gao J, Xie M, Zang X, Liu S, Chen H, Thomas RK, Xue X, Ji H, Chen L. Integrative analysis of multi-omics data reveals the heterogeneity and signatures of immune therapy for small cell lung cancer. Clin Transl Med 2021; 11(12): e620
14. Park S, Hong TH, Hwang S, Heeke S, Gay CM, Kim J, Jung HA, Sun JM, Ahn JS, Ahn MJ, Cho JH, Choi YS, Kim J, Shim YM, Kim HK, Byers LA, Heymach JV, Choi YL, Lee SH, Park K. Comprehensive analysis of transcription factor-based molecular subtypes and their correlation to clinical outcomes in small-cell lung cancer. EBioMedicine 2024; 102: 105062
15. Nabet BY, Hamidi H, Lee MC, Banchereau R, Morris S, Adler L, Gayevskiy V, Elhossiny AM, Srivastava MK, Patil NS, Smith KA, Jesudason R, Chan C, Chang PS, Fernandez M, Rost S, McGinnis LM, Koeppen H, Gay CM, Minna JD, Heymach JV, Chan JM, Rudin CM, Byers LA, Liu SV, Reck M, Shames DS. Immune heterogeneity in small-cell lung cancer and vulnerability to immune checkpoint blockade. Cancer Cell 2024; 42(3): 429–443.e4
16. Bindea G, Mlecnik B, Tosolini M, Kirilovsky A, Waldner M, Obenauf AC, Angell H, Fredriksen T, Lafontaine L, Berger A, Bruneval P, Fridman WH, Becker C, Pagès F, Speicher MR, Trajanoski Z, Galon J. Spatiotemporal dynamics of intratumoral immune cells reveal the immune landscape in human cancer. Immunity 2013; 39(4): 782–795
17. Angelova M, Mlecnik B, Vasaturo A, Bindea G, Fredriksen T, Lafontaine L, Buttard B, Morgand E, Bruni D, Jouret-Mourin A, Hubert C, Kartheuser A, Humblet Y, Ceccarelli M, Syed N, Marincola FM, Bedognetti D, Van den Eynde M, Galon J. Evolution of metastases in space and time under immune selection. Cell 2018; 175(3): 751–765.e16
18. Longo V, Catino A, Montrone M, Pizzutilo P, Annese T, Pesola F, Marech I, Cassiano S, Ribatti D, Galetta D. What are the biomarkers for immunotherapy in SCLC? Int J Mol Sci 2021; 22(20): 11123
19. Li T, Qiao T. Unraveling tumor microenvironment of small-cell lung cancer: implications for immunotherapy. Semin Cancer Biol 2022; 86: 117–125
20. Burr ML, Sparbier CE, Chan KL, Chan YC, Kersbergen A, Lam E, Azidis-Yates E, Vassiliadis D, Bell CC, Gilan O, Jackson S, Tan L, Wong SQ, Hollizeck S, Michalak EM, Siddle HV, McCabe MT, Prinjha RK, Guerra GR, Solomon BJ, Sandhu S, Dawson SJ, Beavis PA, Tothill RW, Cullinane C, Lehner PJ, Sutherland KD, Dawson MA. An evolutionarily conserved function of polycomb silences the MHC class I antigen presentation pathway and enables immune evasion in cancer. Cancer Cell 2019; 36(4): 385–401.e8
21. Zhang X, Guo M, Fan J, Lv Z, Huang Q, Han J, Wu F, Hu G, Xu J, Jin Y. Prognostic significance of serum LDH in small cell lung cancer: a systematic review with meta-analysis. Cancer Biomark 2016; 16(3): 415–423
22. Stratmann JA, Timalsina R, Atmaca A, Rosery V, Frost N, Alt J, Waller CF, Reinmuth N, Rohde G, Saalfeld FC, von Rose AB, Acker F, Aspacher L, Möller M, Sebastian M. Clinical predictors of survival in patients with relapsed/refractory small-cell lung cancer treated with checkpoint inhibitors: a German multicentric real-world analysis. Ther Adv Med Oncol 2022; 14: 17588359221097191
23. Lu Y, Jiang J, Ren C. The clinicopathological and prognostic value of the pretreatment neutrophil-to-lymphocyte ratio in small cell

lung cancer: a meta-analysis. PLoS One 2020; 15(4): e230979
24. Kutlu Y, Aydin SG, Bilici A, Oven BB, Olmez OF, Acikgoz O, Hamdard J. Neutrophil-to-lymphocyte ratio and platelet-to-lymphocyte ratio as prognostic markers in patients with extensive-stage small cell lung cancer treated with atezolizumab in combination with chemotherapy. Medicine (Baltimore) 2023; 102(15): e33432
25. Sonehara K, Tateishi K, Komatsu M, Yamamoto H, Hanaoka M. Lung immune prognostic index as a prognostic factor in patients with small cell lung cancer. Thorac Cancer 2020; 11(6): 1578–1586
26. Xie J, Xu K, Cai Z, Chen M, Jiang Y, Ye J, Lin X, Lv T, Zhan P. Efficacy and safety of first-line PD-L1/PD-1 inhibitors in limited-stage small cell lung cancer: a multicenter propensity score matched retrospective study. Transl Lung Cancer Res 2024; 13(3): 526–539
27. Anpalakhan S, Signori A, Cortellini A, Verzoni E, Giusti R, Aprile G, Ermacora P, Catino A, Pipitone S, Di Napoli M, Scotti V, Mazzoni F, Guglielmini PF, Veccia A, Maruzzo M, Schinzari G, Casadei C, Grossi F, Rizzo M, Montesarchio V, Verderame F, Mencoboni M, Zustovich F, Fratino L, Accettura C, Cinieri S, Tondini CA, Camerini A, Banzi MC, Sorarù M, Zucali PA, Vignani F, Ricciardi S, Russo A, Cosenza A, Di Maio M, De Giorgi U, Pignata S, Giannarelli D, Pinto C, Buti S, Fornarini G, Rebuzzi SE, Rescigno P, Addeo A, Banna GL, Bersanelli M. Using peripheral immune-inflammatory blood markers in tumors treated with immune checkpoint inhibitors: an INVIDIa-2 study sub-analysis. iScience 2023; 26(11): 107970
28. Mezquita L, Auclin E, Ferrara R, Charrier M, Remon J, Planchard D, Ponce S, Ares LP, Leroy L, Audigier-Valette C, Felip E, Zerón-Medina J, Garrido P, Brosseau S, Zalcman G, Mazieres J, Caramela C, Lahmar J, Adam J, Chaput N, Soria JC, Besse B. Association of the lung immune prognostic index with immune checkpoint inhibitor outcomes in patients with advanced non-small cell lung cancer. JAMA Oncol 2018; 4(3): 351–357
29. Zhu Y, Li S, Wang H, Ren W, Chi K, Wu J, Mao L, Huang X, Zhuo M, Lin D. Molecular subtypes, predictive markers and prognosis in small-cell lung carcinoma. J Clin Pathol 2024; 78(1): 42–50
30. Zhu Y, Wu J, Wang H, Chi K, Diao X, Zhuo M, Lin D. Whole-section digital analysis of immune profiles in surgically resected small cell lung carcinoma and their associations with molecular subtypes. Transl Lung Cancer Res 2025; 14(2): 449–466
31. Fedchenko N, Reifenrath J. Different approaches for interpretation and reporting of immunohistochemistry analysis results in the bone tissue - a review. Diagn Pathol 2014; 9(1): 221
32. Qu S, Fetsch P, Thomas A, Pommier Y, Schrump DS, Miettinen MM, Chen H. Molecular subtypes of primary sclc tumors and their associations with neuroendocrine and therapeutic markers. J Thorac Oncol 2022; 17(1): 141–153
33. Iams WT, Porter J, Horn L. Immunotherapeutic approaches for small-cell lung cancer. Nat Rev Clin Oncol 2020; 17(5): 300–312
34. Kulangara K, Zhang N, Corigliano E, Guerrero L, Waldroup S, Jaiswal D, Ms MJ, Shah S, Hanks D, Wang J, Lunceford J, Savage MJ, Juco J, Emancipator K. Clinical utility of the combined positive score for programmed death ligand-1 expression and the approval of pembrolizumab for treatment of gastric cancer. Arch Pathol Lab Med 2019; 143(3): 330–337
35. Bankhead P, Loughrey MB, Fernández JA, Dombrowski Y, McArt DG, Dunne PD, McQuaid S, Gray RT, Murray LJ, Coleman HG, James JA, Salto-Tellez M, Hamilton PW. QuPath: open source software for digital pathology image analysis. Sci Rep 2017; 7(1): 16878
36. Megyesfalvi Z, Barany N, Lantos A, Valko Z, Pipek O, Lang C, Schwendenwein A, Oberndorfer F, Paku S, Ferencz B, Dezso K, Fillinger J, Lohinai Z, Moldvay J, Galffy G, Szeitz B, Rezeli M, Rivard C, Hirsch FR, Brcic L, Popper H, Kern I, Kovacevic M, Skarda J, Mittak M, Marko-Varga G, Bogos K, Renyi-Vamos F, Hoda MA, Klikovits T, Hoetzenecker K, Schelch K, Laszlo V, Dome B. Expression patterns and prognostic relevance of subtype-specific transcription factors in surgically resected small-cell lung cancer: an international multicenter study. J Pathol 2022; 257(5): 674–686
37. Hwang S, Hong TH, Kim HK, Choi YS, Zo JI, Shim YM, Han J, Chan AY, Pyo H, Noh JM, Lee HY, Kim HJ, Park S, Ahn MJ, Park K, Lee SH, Choi YL, Kim J. Whole-section landscape analysis of molecular subtypes in curatively resected small cell lung cancer: clinicopathologic features and prognostic significance. Mod Pathol 2023; 36(7): 100184
38. Zhu Y, Ren W, Li S, Wu J, Hu X, Wang H, Chi K, Zhuo M, Lin D. Heterogeneity of molecular subtyping and therapy-related marker expression in primary tumors and paired lymph node metastases of small cell lung cancer. Virchows Arch 2025; 486(2): 243–255
39. Best SA, Hess JB, Souza-Fonseca-Guimaraes F, Cursons J, Kersbergen A, Dong X, Rautela J, Hyslop SR, Ritchie ME, Davis MJ, Leong TL, Irving L, Steinfort D, Huntington ND, Sutherland KD. Harnessing natural killer immunity in metastatic SCLC. J Thorac Oncol 2020; 15(9): 1507–1521
40. Cai L, Liu H, Huang F, Fujimoto J, Girard L, Chen J, Li Y, Zhang YA, Deb D, Stastny V, Pozo K, Kuo CS, Jia G, Yang C, Zou W, Alomar A, Huffman K, Papari-Zareei M, Yang L, Drapkin B, Akbay EA, Shames DS, Wistuba II, Wang T, Johnson JE, Xiao G, DeBerardinis RJ, Minna JD, Xie Y, Gazdar AF. Cell-autonomous immune gene expression is repressed in pulmonary neuroendocrine cells and small cell lung cancer. Commun Biol 2021; 4(1): 314
41. Tian Y, Li Q, Yang Z, Zhang S, Xu J, Wang Z, Bai H, Duan J, Zheng B, Li W, Cui Y, Wang X, Wan R, Fei K, Zhong J, Gao S, He J, Gay CM, Zhang J, Wang J, Tang F. Single-cell transcriptomic profiling reveals the tumor heterogeneity of small-cell lung cancer. Signal Transduct Target Ther 2022; 7(1): 346
42. Muppa P, Parrilha TS, Sharma A, Mansfield AS, Aubry MC, Bhinge K, Asiedu MK, de Andrade M, Janaki N, Murphy SJ, Nasir A, Van Keulen V, Vasmatzis G, Wigle DA, Yang P, Yi ES, Peikert T, Kosari F. Immune cell infiltration may be a key determinant of long-term survival in small cell lung cancer. J Thorac Oncol 2019; 14(7): 1286–1295
43. Shirasawa M, Yoshida T, Shiraishi K, Takigami A, Takayanagi D, Imabayashi T, Matsumoto Y, Masuda K, Shinno Y, Okuma Y, Goto Y, Horinouchi H, Yotsukura M, Yoshida Y, Nakagawa K, Tsuchida T, Hamamoto R, Yamamoto N, Motoi N, Kohno T, Watanabe SI, Ohe Y. Identification of inflamed-phenotype of small cell lung cancer leading to the efficacy of anti-PD-L1

antibody and chemotherapy. Lung Cancer 2023; 179: 107183
44. Thomas A, Vilimas R, Trindade C, Erwin-Cohen R, Roper N, Xi L, Krishnasamy V, Levy E, Mammen A, Nichols S, Chen Y, Velcheti V, Yin F, Szabo E, Pommier Y, Steinberg SM, Trepel JB, Raffeld M, Young HA, Khan J, Hewitt S, Lee JM. Durvalumab in combination with olaparib in patients with relapsed SCLC: results from a phase II study. J Thorac Oncol 2019; 14(8): 1447–1457
45. Pasello G, Lorenzi M, Tosi A, Roma A, Pavan A, Scapinello A, Lonardi S, Ferro A, Maso AD, Frega S, Bonanno L, Del Bianco P, Guarneri V, Rosato A. 164P Immune cells distribution and spatial relationship within microenvironment as predictive biomarkers of benefit in extended stage small cell lung cancer patients receiving atezolizumab plus carboplatin and etoposide as first-line treatment. J Thorac Oncol 2023; 18(4): S130
46. Hiam-Galvez KJ, Allen BM, Spitzer MH. Systemic immunity in cancer. Nat Rev Cancer 2021; 21(6): 345–359